CPT: Pharmacometrics & Systems Pharmacology

ARTICLE OPEN ACCESS

Using Pharmacokinetic and Pharmacodynamic Analysis to Optimize the Dosing Regimens of Fanastomig (EMB-02) in Patients With Advanced Solid Tumors

Chengjun Jiang | Fang Ren | Mingfei Zhang | Qiaoyang Lu | Shuqi Zeng | Guang Yang | Yonghong Zhu

Hanghai EpimAb Biotherapeutics Co., Ltd, Shanghai EpimAb Biotherapeutics, Shanghai, China

Correspondence: Chengjun Jiang (chjjiang@epimab.com) | Yonghong Zhu (yhzhu@epimab.com)

Received: 28 November 2024 | **Revised:** 11 February 2025 | **Accepted:** 14 February 2025

Funding: This study was provided by Shanghai EpimAb Biotherapeutics Co., Ltd.

Keywords: dose optimization | exposure and response | Fanastomig | lympahocyte activation gene-3 (LAG-3) | population pharmacokinetic model | programmed cell death protein 1 (PD-1) | receptor occupancy

ABSTRACT

Fanastomig (also known as EMB-02) is a bispecific antibody targeting programmed cell death protein-1(PD-1) and lymphocyte activation gene-3 (LAG-3), developed for the treatment of advanced solid tumors. A first-in-human (FIH) Phase I study (NCT04618393) evaluated safety, tolerability, pharmacokinetics (PK), pharmacodynamics (PD), immunogenicity, and clinical efficacy of Fanastomig in patients with advanced solid tumors. To determine the recommended Phase II dose (RP2D), population pharmacokinetics (PopPK), and exposure and response analysis (E-R) were conducted. The PopPK model, demonstrating good performance, showed no clinically meaningful relationship between areas under the concentration–time curve (AUC) or maximum concentration (C_{max}) of Fanastomig and selected covariates of interest. A nonlinear E_{max} model was fitted to Fanastomig PD-1 receptor occupancy (RO) in the peripheral blood compartment. The estimated half-maximal effective concentration (EC_{50}) was 0.084 μg/mL (95% confidence interval [CI]: 0.0369–0.131). Assuming a threefold lower exposure in tumor tissue compared to that in serum, a target trough concentration of Fanastomig at ~2.27 μg/mL would be needed for 90% PD-1 RO in the tumor. Modeling and simulation indicated that a weekly dosing (QW) of 360 mg would achieve full peripheral blood RO in approximately 90% of patients. The incidence of anti-drug antibodies (ADAs) for Fanastomig was high (95.7%, 44/46), with a negative correlation between the ADA titer and dose levels; meanwhile, ADA minimally impacted PK exposure and efficacy. An inverse trend was observed between anaphylaxis and PK exposure. Fanastomig was well tolerated and had acceptable safety profiles up to 900 mg QW. Based on these findings, two dosing regimens have been selected for further clinical development.

Trial Registration: ClinicalTrials.gov identifier: NCT04618393

1 | Introduction

In a first-in-human (FIH) study in oncology, identifying the appropriate dose and dosing interval for Phase II trials is one of the main investigative aims. However, small sample size, typically heterogeneous study population, and limited efficacy events often present significant challenges for selecting the appropriate dosing regimen (s) in FIH study [1–3]. For some targeted anticancer agents, higher yet efficacious doses lead to off-target effects including toxicity, dose interruptions, and reduced compliance, while optimized lower yet efficacious doses result in good antitumor responses with much lower toxicity and better drug compliance [2, 4]. Model-based data analysis, which integrates the preclinical data and clinical data, is a powerful tool for extracting maximal information to inform the dosing regimen(s) selection [5, 6]. In the early process of oncology drug

Summary

- What is the current knowledge on the topic?
  - Fanastomig is a bispecific antibody designed to simultaneously target the immune checkpoints programmed cell death protein-1 (PD-1) and lymphocyte activation gene-3 (LAG-3). By blocking both PD-1 and LAG-3, it has the potential to enhance antitumor immunity by overcoming resistance mechanisms often associated with monotherapies targeting a single checkpoint. Fanastomig has been evaluated in a first-in-human (FIH) study to assess its safety, pharmacokinetics (PK), pharmacodynamics (PD), and clinical efficacy, with PK/PD data integration to inform dosing regimen strategies.
- What questions did this study address?
  - This study aimed to use population PK/PD modeling and simulation to characterize the PK profile of Fanastomig, understand its pharmacodynamic effects through PD-1 receptor occupancy (RO), assess the impact of anti–drug antibodies (ADAs) on PK, safety, and efficacy, and ultimately propose optimized dosing regimens for Phase II clinical trials in patients with advanced solid tumors.
- What does this study add to knowledge?
  - The study established a two-compartment population pharmacokinetic (PK) model with time-dependent linear elimination for Fanastomig, revealing no covariate effects on PK parameters. Evaluation of PD-1 receptor occupancy (RO) and the corresponding target concentration of Fanastomig in tumors supported two dosing regimens: 180 mg weekly for 8 weeks, followed by 360 mg every 2 weeks, and 300 mg weekly for 8 weeks, followed by 600 mg every 2 weeks. These regimens are predicted to maintain therapeutic concentrations while balancing safety considerations.
- How might this change drug discovery, development, and/or therapeutics?
  - This study underscores the value of model-informed drug development (MIDD) in optimizing dosing regimens for complex biologics like bispecific antibodies in early-phase oncology trials. By integrating PK/PD modeling with receptor occupancy (RO) data and considering immunogenicity factors, the research provides a systematic approach to dose selection that moves beyond traditional maximum tolerated dose (MTD) paradigms. The findings highlight that high ADA incidence does not necessarily compromise drug efficacy or alter PK profiles significantly, offering insights into managing immunogenicity in multispecific antibody development.

development, particularly for targeting molecular pathways, the Food and Drug Administration (FDA) and other health authorities have advocated the model-informed drug development (MIDD) paradigm over the traditional maximum tolerated dose (MTD) approach [4, 7]. The shift from the MTD paradigm to the MIDD approach in dose selection has been increasingly emphasized during recent years [8].

In the MIDD approach, a reliable pharmacodynamics (PD) biomarker can provide informative surrogate data to characterize the relationship between drug exposure and efficacy or safety. For certain cellular-targeted agents, immune parameters and receptor occupancy (RO) are critical PD readouts in drug development, helping to establish minimum biological effect dose regimens. For example, in the immune oncology field, the $CD3^+$, $CD8^+$, or $CD45^+/CD3^+$ were measured as T-cell markers for programmed cell death protein-1 (PD-1) blockage in several published studies [9–11].

Using PD-1 RO as a basis for comparing alternative dosing regimens is a widely accepted approach in immune-oncology, as it partially reflects the mechanism of action, which involves immune checkpoint blockade, of this class of drug. Nivolumab data show that receptor occupancy exceeds 65% at doses ≥ 0.3 mg/kg, with the 3 mg/kg dose approved for monotherapy across most indications [12, 13]. Pembrolizumab data show that receptor saturation $> 95\%$ is achieved at doses ≥ 1 mg/kg, with the 2 mg/kg dose approved for monotherapy in most indications [13, 14]. Furthermore, an FDA guideline indicates that receptor occupancy data can be used to support changes in dosing regimens [15]. Although a good correlation between peripheral blood RO and tumor RO has been reported in preclinical models [16], practical challenges such as tumor heterogeneity and the tumor microenvironment (TME) must be fully considered when interpreting these biomarkers [17, 18].

This article describes the application of integrated population PK/PD modeling of the FIH dose escalation data to optimize the dosing regimens for Fanastomig, a symmetric IgG-like bispecific antibody against PD-1 and LAG-3. Dual blockade of PD-1 and LAG-3 in the TME, where they can be co-expressed on the same T cells, affords the opportunity to maximize immune checkpoint blockade while limiting systemic toxicity [19]. To reduce potential effector function induced depletion of immune cells expressing PD-1 or LAG-3, Fanastomig was specifically designed with decreased effector function by the Fabs-In-Tandem Immunoglobulin (FIT-Ig) platform, in which the human IgG1 Fc domain of Fanastomig was engineered to contain a LALA double mutation (mutation of leucine residues at positions 234 and 235 into alanine residues) [20].

In this study, a total of 47 patients with various metastatic or advanced solid tumors received Fanastomig at dose levels ranging from 6 to 900 mg once weekly (QW). The overall response (ORR) was 6.4%, with 3 patients achieving the best overall response (BOR) of confirmed complete response (CR)—one in the 6 mg group and two in the 60 mg group—and no patients achieving BOR of partial response (PR). With 18 (38.3%) patients having a BOR of stable disease (SD), the disease control rate (DCR) was 44.7% (21/47). The MTD was not reached for Fanastomig; only one dose-limiting toxicity (DLT) event (Grade 4 immune-mediated hepatitis) occurred at 900 mg in five patients. No other significant safety concerns were observed at doses below 900 mg QW. The most frequent treatment-related adverse events (AEs) were infusion-related reaction (IRR), fatigue, and diarrhea [In press].

Here, we report the first PopPK, exposure efficacy, and exposure-safety analysis of the Fanastomig. The analysis evaluates the

impact of intrinsic and extrinsic factors on the PK of Fanastomig and explores the PK exposure levels required to maintain full PD-1 receptor occupancy in tumors, thereby helping to identify potentially effective doses.

2 | Methods

2.1 | Study Design and Objectives

This was a FIH, open-label, dose escalation study conducted in patients with advanced solid tumors enrolled from China, the United States, and Australia. The primary objective of this study was to evaluate the safety and tolerability of Fanastomig and to determine the MTD and/or recommended Phase 2 doses (RP2Ds). The secondary objectives included characterizing the PK profile, assessing preliminary antitumor activity using Response Evaluation Criteria in Solid Tumors (RECIST) version 1.1, and characterizing the anti-drug antibody (ADA) of Fanastomig.

The study consisted of two parts. Part 1 was the dose escalation stage, exploring safety, tolerability, preliminary efficacy signal, PK, and PD profiles of Fanastomig at dose levels ranging from 6 to 900 mg, administered QW. Part 2 was the dose enrichment stage, with expansion at dose levels of 60, 180, and 600 mg.

The study was conducted in accordance with the Declaration of Helsinki and Good Clinical Practice guidelines (GCP). The protocol was approved by the ethics committee at each investigational site, and all participants provided written informed consent prior to enrollment.

2.2 | Dose Regimen and Sample Analysis

In the development of the PopPK model, all patients who received at least one dose of Fanastomig and had at least one PK sample were included in the PK population for model development. Fanastomig dose regimens included 6, 20, 60, 180, 360, 600, and 900 mg administered QW in Part 1, and 60, 180, and 600 mg QW in Part 2. Serum samples were analyzed for Fanastomig concentration using an enzyme-linked immunosorbent assay (ELISA). PD biomarker PD-1 RO was measured in blood samples using a flow cytometry assay. Serum ADAs against Fanastomig were detected using an electrochemiluminescence method.

2.3 | PopPK Model Development

The PopPK model of Fanastomig was developed using the nonlinear mixed effects (NLME) modeling software Phoenix NLME Version 8.0 (Certara USA Inc., Princeton, NJ, USA), employing the first-order conditions estimate (FOCE) method. Model development followed a three-step process: (1) establishment of a basic structural model that adequately described the PK profiles of Fanastomig in the population; (2) identification of significant covariates explaining interindividual variability (IIV) in the PopPK model; (3) development of the final PopPK model by incorporating significant covariates into the base model.

In the assessment of the structural model, various models were evaluated, including two-compartment models incorporating linear, nonlinear, and parallel linear/nonlinear clearance (CL) mechanisms. Additionally, time-dependent CL was considered, with the sigmoid maximal inhibitory clearance model being applied (Equation 1), as observed with other immune checkpoint inhibitors such as nivolumab, atezolizumab, and durvalumab [21–24]. Furthermore, a simpler exponential decay model (Equation 2), both as a standalone model and in combination with time-independent or nonlinear CL, was also investigated.

$$\mathrm{CL}_{i,t} = \mathrm{TVCL} * \exp\left(\frac{I_{\max,i} * t_i^{\mathrm{Hill}}}{T_{50}^{\mathrm{Hill}} + t_i^{\mathrm{Hill}}}\right) \quad (1)$$

$$CL_{i,t} = \mathrm{TVCL} * \exp\left(-K_{\mathrm{des}} * t_i\right) \quad (2)$$

where, $\mathrm{CL}_{i,t}$ represents CL of the ith individual at time t. TVCL denotes the typical value of CL at Time = 0. $I_{\max,I}$ indicates the maximal change in CL relative to baseline CL for the ith individual, and T_{50} is the time at which the change is half of its maximum in CL, while Hill is an exponential shape parameter. K_{des} is the decay coefficient of time-dependent clearance.

The following exponential random-effects models were employed to characterize the inter-individual variability (Equation 3) and proportional residual models were employed to characterize the residual variability (Equation 4)

$$\theta_i = \theta * exp(\eta_i) \quad (3)$$

$$\mathrm{C}_{i,j} = \mathrm{C} * \left(1 + \varepsilon_{ij}\right) \quad (4)$$

where θ is the population typical value and ηi is the deviation from the typical for the ith subject with a mean of zero and variance ω2. The approximate percent coefficient of variation (%CV) was reported (Equation 5). Where C_{ij} is the jth measured observation for the ith subject and $\varepsilon_{\mathrm{p}ij}$ is the proportional residual random error, for an individual i and measurement j.

$$\%\,\mathrm{CV} = \sqrt{\omega 2} \times 100\,\% \quad (5)$$

Covariates were evaluated for their effect on Fanastomig PK parameters using a stepwise covariate modeling (SCM) strategy. Based on the predefined criteria and graphical evaluation from the base model, the relationship between continuous covariates and PK parameters was described using power models (Equation 6) while categorical covariates were tested using a linear function (Equation 7)

$$\mathrm{Par}_i = \mathrm{Par}_{\mathrm{ref}} * \left(\frac{\mathrm{COV}i}{\mathrm{COV}_{\mathrm{med}}}\right)^{\theta \mathrm{Par,Cov}} \quad (6)$$

$$\mathrm{Par}_i = \mathrm{Par}_{\mathrm{ref}} * \left(1 + \theta_{\mathrm{Par,Cov}}\right) \quad (7)$$

Par_i is the parameter value for the ith individual, and $\mathrm{Par}_{\mathrm{ref}}$ is the parameter value when the covariate was the standard reference value or median value. Cov$i$ is the covariate value of the ith individual, and $\mathrm{Cov}_{\mathrm{med}}$ is the covariate median value in the population. θ (Par, Cov) is a parameter describing the covariate effect on the parameter.

The Stepwise covariate modeling was conducted using a change in objective function value (OFV) of 6.63 ($p < 0.01$) for forward inclusion and 10.8 ($p < 0.001$) for backward elimination. The stability and predictive performance (i.e., precision and accuracy) of models were evaluated using Objective function value (OFV), Bayesian information criteria (BIC), Akaike information criterion (AIC), relative standard error (RSE), goodness-of-fit plots (GOF), and the normalized prediction distribution (NPD), visual predictive checks (VPCs) and prediction-corrected VPC (pcVPC). Additionally, the physiological plausibility of the parameter estimates and successful numerical convergence were ensured.

Forest plots that illustrate the effect of covariates on exposure metrics at steady state were generated based on simulations with uncertainty in fixed-effect parameters. The reference condition was the approximate median value, and the test conditions were the 5th and 95th percentiles for continuous covariates. For categorical covariates, the conditions were the same mode of the final model. A total of 1000 sets of fixed-effect parameters were sampled from the estimated value.

2.4 | Receptor Occupancy Assessment

To evaluate the PD effect of Fanastomig, RO of PD-1 and LAG-3 on peripheral blood $CD3^+$, $CD4^+$, and $CD8^+$ T cells were measured. Blood samples for PD biomarkers were collected predose on Cycle 1 Day (C1D1), 48 h post-first infusion (±1 h), and prior to dosing on C1D8, C1D15, C1D22, C2D1, C3D1, and C4D1. PD-1 RO in each sample was measured using a validated flow cytometry assay. Due to the very low expression level of LAG-3 on peripheral blood T cells, LAG-3 RO could not be accurately calculated. All PD-1 RO data were included in a nonlinear E_{max} model to estimate the EC_{50} value.

2.5 | Assessment of ADA and Exploratory Analysis of ADA Titer Effects on PK, Safety, and Efficacy

ADA data were collected from 46 evaluable patients who had at least both ADA test readouts at baseline and any time post-first dose. All samples are analyzed in a screening assay, with positive samples being tested in a confirmatory assay and typically further characterized to assess ADA titer. The ADA titer for each positive sample was determined by analyzing serial dilutions. The effect of ADA titer on PK, safety, and efficacy was evaluated. Exploratory boxplots were generated to investigate the relationship between ADA titer and PK, safety, and efficacy metrics, with statistical evaluation performed using the Wilcoxon test.

2.5.1 | ADA Titer and PK Analysis

The ADA titer and PK analysis included 30 out of 46 patients (65.2%) who had both ADA results prior to C2D1 and PK parameters available at C2D1. Patients who developed ADA positive were grouped based on their maximum ADA titer values. The median value of the maximum titer among ADApositive patients was 56.96. Patients were classified into three groups: the ADA negative group ($n = 5$), the low ADA titer group ($n = 13$), which included patients with a maximum ADA titer below 56.96, and the high ADA titer group ($n = 12$), which consisted of patients with a maximum ADA titer ≥ 56.96.

2.5.2 | ADA Titer and Safety/Efficacy Analysis

Some studies have reported that patients who are ADA-positive may experience anaphylactic reactions. Anaphylaxis is conventionally considered an immunoglobulin E (IgE)-mediated reaction, involving symptoms such as hypotension, bronchospasm, laryngeal or pharyngeal edema, wheezing, and/or urticaria [25, 26]. Therefore, safety parameters for anaphylaxis—including infusion-related reaction (IRR), hypotension, wheezing, and urticaria related to Fanastomig—were analyzed using preferred term codes from the Medical Dictionary for Regulatory Activities (MedDRA) Version 23.0. The relationship between ADA titer and treatment-related AEs of anaphylaxis was assessed by evaluating the statistical significance (p value) of the association between ADA titer and the binary occurrence of anaphylactic events (responder and nonresponder). Patients with both positive ADA results and symptoms of anaphylaxis were included in this analysis. A total of 44 patients were categorized into responder and nonresponder groups based on the presence or absence of anaphylactic reactions. The impact of ADA titer on treatment efficacy was evaluated using the same method as for safety. This assessment aimed to understand the correlation between ADA levels and clinical effectiveness.

2.6 | E-R Analysis

Exposure-safety and exposure-efficacy datasets were constructed for patients administered IV Fanastomig who had evaluable efficacy or safety data, along with post hoc estimated PK exposure parameters from the final PopPK model. To explore the relationship between Fanastomig exposure and safety/efficacy, we examined the correlation between under area concentration–time curve (AUC) and maximum concentration (C_{max}) with the incidence of anaphylaxis. Additionally, AUC and C2D1 trough concentration (C_{trough}) were included in a correlation analysis of the best tumor size change from baseline. The analysis was performed using R software (version 4.3.3).

3 | Results

3.1 | PopPK Model Characterization, Evaluation, and Influence of Covariate on Exposure

A total of 950 PK observations from 47 patients were initially considered for the development of the PopPK model. However, 249 PK observations from 12 patients were excluded because these patients had been pretreated with PD-1 inhibitors within 4 months prior to initiating the Fanastomig treatment and exhibited higher predose concentrations of anti-PD(L)1 antibody. Additionally, 71 below quantification limit (BQL) values—33 samples collected prior to the first dose and 38 samples collected

post treatment—were excluded during the model development stage, with 5 outlier values also excluded in the model development stage. As a result, 625 PK observations concentrations were utilized in the final model. Baseline demographics and clinical characteristics used as covariates in the PopPK model are summarized in Table S1.

The list of the structure model development is provided in Table S2. The covariate screening results and the outcomes of stepwise covariate modeling for the covariate model are presented in Figure S1 and Appendix S1, respectively. Table 1 presents the final population PK parameters estimates along with their precision and the results of the bootstrap validation procedure. The concentration–time profile of Fanastomig was well described by a two-compartment model with time-dependent linear elimination. The time dependency in clearance (CL) was best characterized empirically by a sigmoid I_{max} function, with a maximum reduction of 61.5%.

The relative standard error (RSE%) for each fixed effects parameter estimate was < 30%, indicating acceptable precision. Relatively large RSE% values were observed for IIV, ranging from 24.0% to 43.77%, while the residual variability, described by a proportional error model, was 7.36%. The median value of the PopPK parameter estimates obtained from the bootstrap procedure was similar to those derived from the final population model, suggesting that the final model reliably estimates the parameters. The model-estimated median half-life was 3.7 days.

Across the range of Fanastomig doses, the final model demonstrated appropriate agreement between observed and model prediction values, indicating that the model estimated PK parameters with sufficient precision. The conditional weighted residual (CWRES) from the GOF plot (Figure S2) was randomly scattered around zero across the predicted range and over time. The VPC plot (Figure 1) and pcVPC (Figure S3) indicated that the vast majority of DV were contained within the final model-based simulation confidence intervals, indicating the model had good prediction performance. The NPD was considered a normal distribution and variance homogeneity, and the NPD versus time or prediction had no apparent tendency to deviate from specified intervals (Figure S4). Overall, the final model adequately predicted the Fanastomig concentration vs. time profile across doses. The final model code can be found in Appendix S1.

The final PopPK model included the covariate effects of albumin. Forest plots of the impacts of covariates on exposure at steady state in the final model are shown in Figure 2. As with AUC, the impacts of ALB covariates were within the no-effect range of 80%–125% of the point estimate of the covariates. However, patients with a lower ALB level had a reduction of 25% in C_{max}. The VPC plot stratified by ALB demonstrated consistent trends across all strata (Figure S5).

TABLE 1 | Estimation of PK parameters in the best final model and bootstrap procedure.

	Final model			Bootstrap ($n = 500$)	
Parameter	**Estimated**	**RSE (%)**	**95% CI**	**Median**	**95% CI**
Fixed effect parameter					
V_c (L)[a]	5.20	4.52	4.73–5.66	5.17	4.73–5.72
V_p (L)	3.15	12.1	2.40–3.90	3.14	2.39–4.03
CL (L/h)[a]	0.215	5.76	0.190–0.239	0.215	0.194–0.242
Q (L/h)	0.0463	12.5	0.0350–0.0576	0.0461	0.036–0.0603
I_{max}[a]	−0.954	−12.6	−1.19 to −0.717	−0.959	−1.21 to-0.732
Hill	8.49	28.6	7.73–13.3	8.68	4.54–72.5
T_{50} (h)[a]	180	9.24	147–213	178	148–227
Effect of ALB on V_p	−0.924	−19.2	−1.27 to-0.576	−0.952	−1.34 to −0.567
Interindividual variability					
IIV (ω^2Vc)	0.035	34.4	0.0113–0.0584	0.0316	0.00791–0.0544
IIV (ω^2 Cl)	0.068	24.0	0.0360–0.1002	0.0664	0.0323–0.101
IIV ($\omega^2 I_{max}$)	0.416	28.1	0.187–0.645	0.402	0.166–0.639
IIV ($\omega^2 T_{50}$)	0.394	43.77	0.056–0.713	0.386	0.0116–0.760
Residual variability					
Prop (σ)	0.378	7.36	0.323–0.433	0.378	0.320–0.429

Note: The shrinkage was calculated using the following equation: η-shrinkage = 1−SD (η)/ω.
Abbreviations: ALB, albumin; CI, confidence interval; CL, apparent systemic clearance; IIV, interindividual variability; I_{max}, maximal decrease in clearance relative to baseline; Prop, proportional part of the residual error variance; Q, inter-compartment clearance; RSE, relative standard error; T_{50}, time at which 50% of I_{max} is reached; V_c, central volume of distribution; V_p, peripheral volume of distribution; σ, standard deviations of sigma; ω^2, variance of omega.
[a]Shrinkage estimates: 27.0% for IIV in V_c, 11.6% for IIV in CL, 9.2% for IIV in I_{max} and 21.6% for IIV in T_{50}.

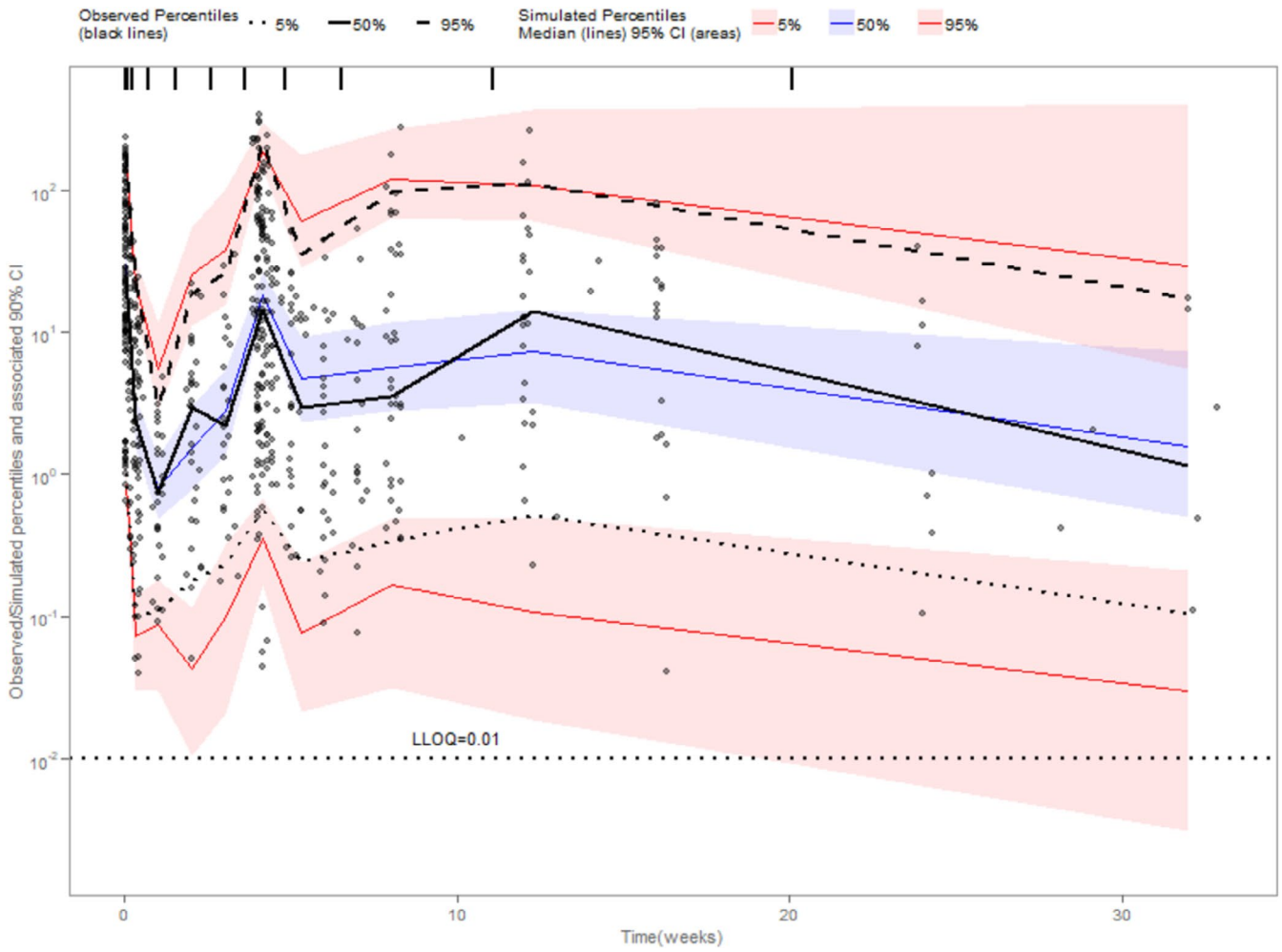

FIGURE 1 | Visual predictive check (VPC) for logarithmic-transformed observations of Fanastomig. The black points represent observed concentration, while the dark-red dotted lines represent the 5th, 50th, and 95th percentiles of predicted concentrations. The dashed black lines show the 5th, 50th, and 95th percentiles of observed concentrations, and the shaded regions represent the 95% CIs for the medians (solid red lines), respectively.

3.2 | Receptor Occupancy

Based on the observed data, Fanastomig showed dose-dependent PD-1 RO across the 6–360 mg dose cohort. Complete occupancy of PD-1 receptors was achieved at doses ≥ 360 mg of Fanastomig. The available RO data, based on $CD3^+$ T cells, were fitted to an E_{max} model as a function of Fanastomig concentration. The EC_{50} for peripheral PD-1 RO was approximately 0.084 μg/mL (Figure 3). Based on this EC_{50} value, a target Fanastomig concentration of 0.756 μg/mL is needed to maintain 90% of maximal peripheral PD-1 RO. Considering a typical threefold dilution factor for penetration into tumor tissues, a concentration of 2.27 μg/mL would be required to achieve 90% PD-1 RO within the tumor [27–29].

3.3 | Predicted Exposure

Predicted Fanastomig concentration versus time profiles for patients were simulated using individual post hoc PK parameter estimates from the final model. Both the target serum exposure of Fanastomig, estimated in an E_{max} model of the peripheral RO data and clinical pharmacokinetic data obtained from patients, indicated that a 360 mg QW regimen would be sufficient to maintain the trough concentration above the preliminary established target concentration of 2.27 μg/mL (Figure 4). This indicates that this dosing regimen should be further explored in more patients to assess its efficacy and safety.

However, considering recent findings regarding patient adherence and the convenience of the dosing regimen, alternative dosing strategies were evaluated to enhance the overall treatment experience and ensure the utilization of the optimal dose in oncology. To achieve this, we evaluated multiple dosing regimens to identify more convenient dosing schemes for a broader patient population, thereby facilitating drug development.

The first alternative regimen involved an initial phase of 300 mg QW for eight doses, followed by 600 mg Q2W. Simulation data indicated that most patients reached target concentration levels after the fifth 300 mg QW dose, with nearly 70% maintaining these levels after the fourth 600 mg Q2W dose (a total of 12 doses). The second regimen started with 180 mg QW for eight doses, followed by 360 mg Q2W. In this case, simulations showed that approximately 70% of patients reached target concentration levels after the fifth 180 mg QW dose, with approximately 50% of patients maintaining these levels after the fourth 360 mg Q2W

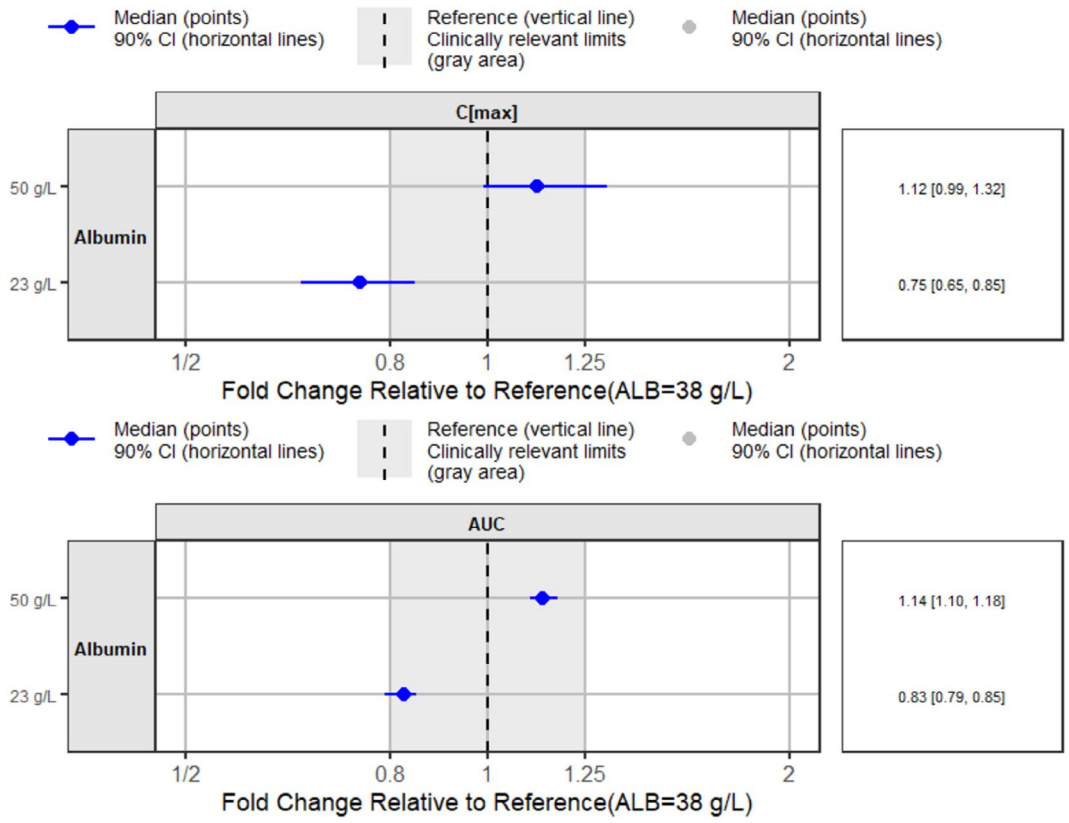

FIGURE 2 | Forest plot of the impact of covariate (ALB) on Fanastomig exposure according to the final PopPK model.

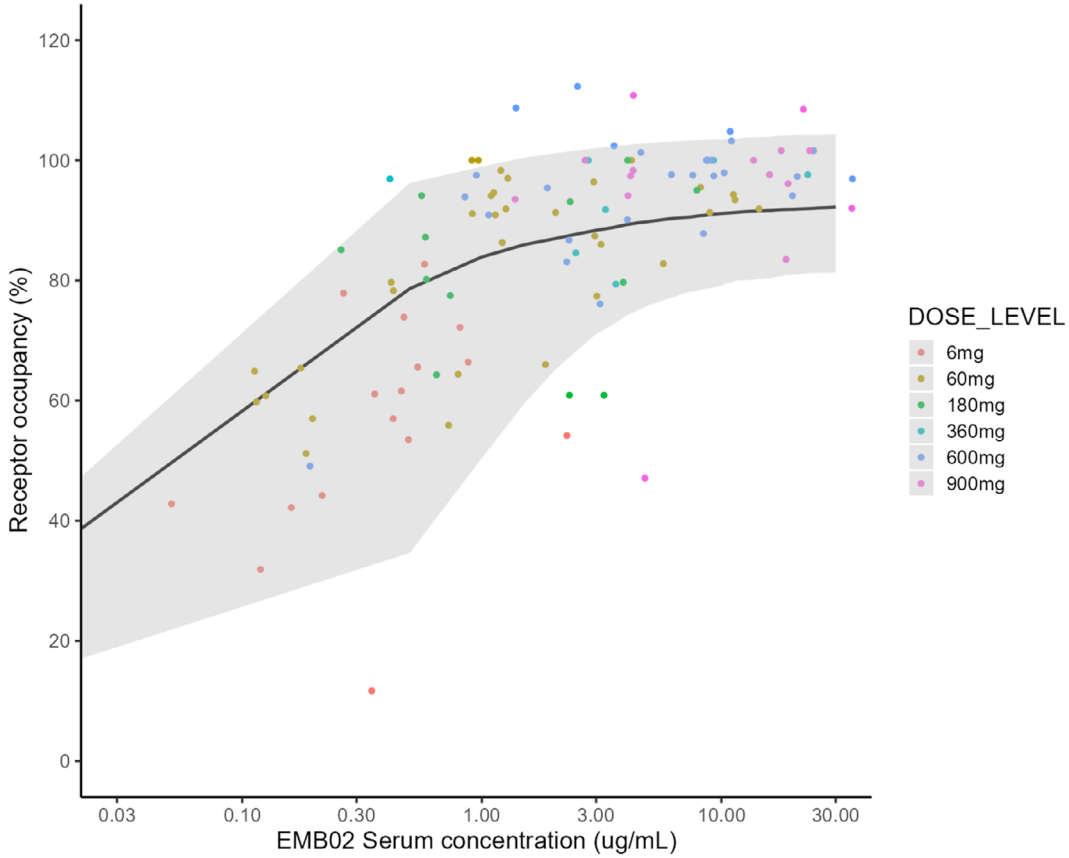

FIGURE 3 | Receptor occupancy and Fanastomig serum concentration analysis for simulated patients ($n = 1000$). The gray ribbon represents the range between the 5th percentile and the 95th percentile, while the black line represents the 50th percentile. Observed RO values at different dose levels are indicated by different colors.

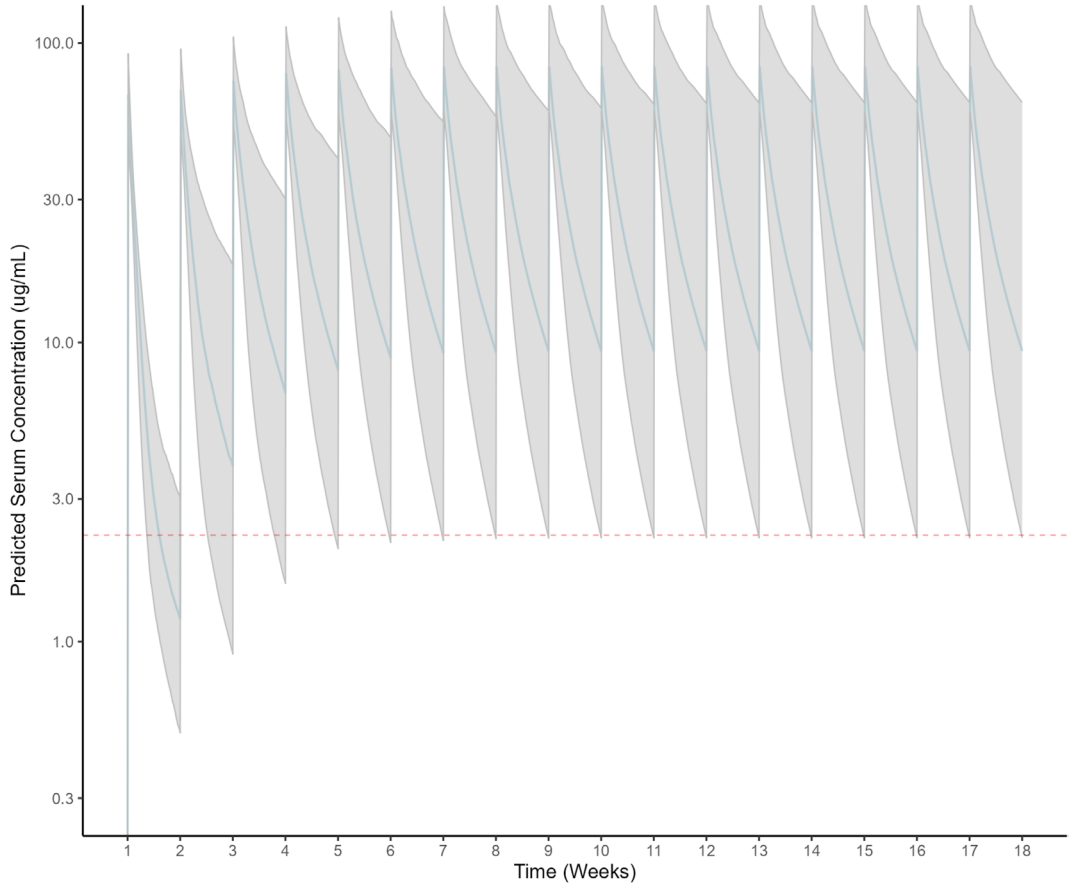

FIGURE 4 | Simulated Fanastomig serum concentration-time profiles following IV administration of 360 mg QW using the final PopPK model and post hoc estimates of parameters. The light gray ribbon represents the range between the 5th percentile and the 95th percentile, and the blue line represents the median (50th percentile). The dash red line represents target exposure (~2.27 μg/mL) derived E_{max} model.

dose (a total of 12 doses) (Table S3). The comparison of the median serum concentration–time profiles following the 360 mg QW and alternative regimens (180 QW for 8 weeks followed by 360 mg Q2W and 300 QW for 8 weeks followed by 600 mg Q2W) is displayed in Figure S6.

3.4 | Immunogenicity Evaluation and Exploratory Analysis of Effect of ADA Titer on PK, Safety, and Efficacy

The preliminary immunogenicity assessment of Fanastomig indicated a relatively high incidence of ADAs, with 44 out of 46 (95.7%) evaluable patients showing positive results. The median onset time for ADA development was 14 days. A summary of ADA data is presented in Table S4. A boxplot of maximum ADA titer versus dose levels demonstrated an inverse relationship: higher titers were observed at 6 and 20 mg doses, whereas doses exceeding 60 mg generally resulted in lower ADA titers (Figure 5a).

3.5 | ADA Titer and PK Analysis

Patients who experienced high ADA titer had a marginally lower median CL compared to those with low ADA titer and ADA negative status, indicating a significant difference with $p > 0.016$. The result of the analysis suggests that, based on the limited data, the CL was not substantially affected by ADA titer (Figure 5b).

3.6 | ADA Titer and Safety (Anaphylaxis)/Efficacy Analysis

Patients who experienced anaphylaxis had a visibly higher median ADA titer compared to those who did not, indicating a significant difference with $p = 0.0068$ (Figure 5c). The significant increase in ADA titer among these patients suggests the possibility of a heightened immune response, which may contribute to the observed anaphylactic reactions.

Both responders and nonresponders, in terms of DCR, exhibited similar median ADA titer, with no significant difference ($p = 0.9$) (Figure 5d). This similarity suggests that ADA presence may not be a distinguishing factor for DCR, although the limited number of patients warrants cautious interpretation.

3.7 | Exposure-Safety/Efficacy Relationship

Logistic regression analysis was conducted to evaluate the exposure–safety relationship, focusing on the most prevalent drug-related AE of anaphylaxis. Exposure metrics at C2D1 for the

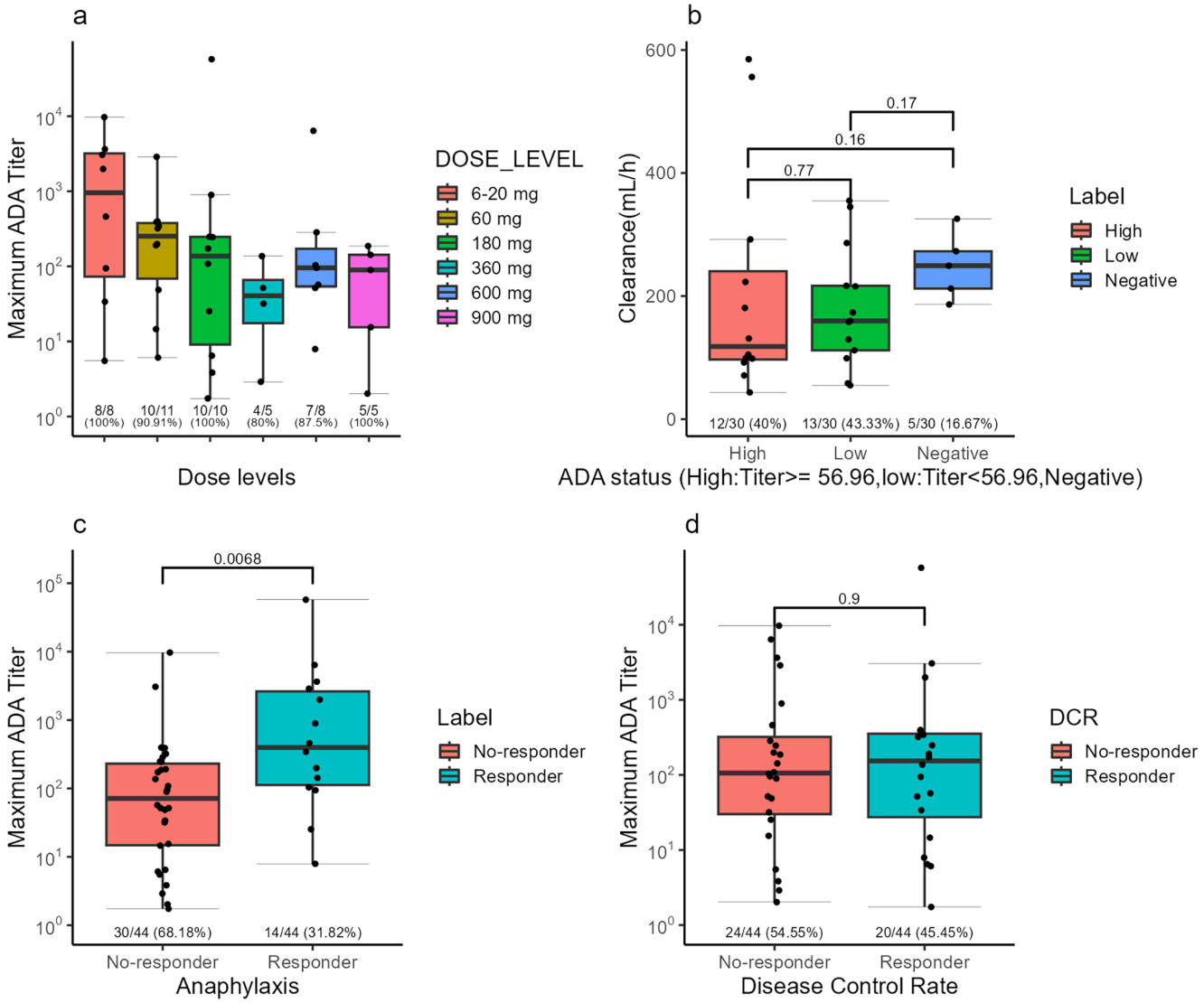

FIGURE 5 | ADA assessment, (a) Influence of dose cohorts on ADA titer. (b) Influence of ADA on PK (Clearance rate). (c) Influence of ADA on safety (Anaphylaxis). (d) Influence of ADA on efficacy (Disease control rate).

patients included in the ER analysis of safety ($n = 35$) indicated that there was a negative trend between AUC or C_{max} and the incidence of anaphylaxis (Figure 6a,b), this trend was not a statistically significant relationship ($p > 0.05$).

Correlation analysis was performed to assess the relationship between exposure and efficacy, measured by the best change in tumor size from baseline. Exposure metrics at C2D1 for the patients included in the efficacy analysis ($n = 27$) showed a nearly flat trend between C_{trough} or AUC and the best change in tumor size (Figure 6c,d), with no statistically significant relationship ($p > 0.05$).

4 | Discussion

This analysis represents the first evaluation of the PopPK of Fanastomig, based on interim data collected in the completed Phase 1 part of the EMB02X101 trial in patients with advanced solid tumors. The PK profile of Fanastomig was well described by a two-compartment model with a time-dependent linear elimination. Both time-varying CL and a linear elimination pattern have previously been observed for Immune Checkpoint Inhibitors (ICIs) within their therapeutic dose range [30]. However, while Fanastomig demonstrated time-varying CL, the magnitude of this change was higher compared to observations for other PD-1 inhibitors. Specifically, the typical maximum reduction in Fanastomig CL over time was estimated at 61.5%, which is higher than that reported for pembrolizumab (20%–30%), nivolumab (~25%), or dostarlimab (14.9%) [30–33]. Furthermore, the Hill parameter (8.49) was slightly higher compared to other PD-1 inhibitors, indicating a relatively steep time-CL relationship. This phenomenon has largely been attributed to disease status, whereby CL decreases as tumor burden declines [32]. Improvement in tumor burden reduces the amount of available surface targets and hence limits the capacity for target-mediated degradation of ICIs [32]. The observed differences in the maximum change in CL over time between agents may be due to variations in study sampling schemes and the proportion of available patients undergoing long-term

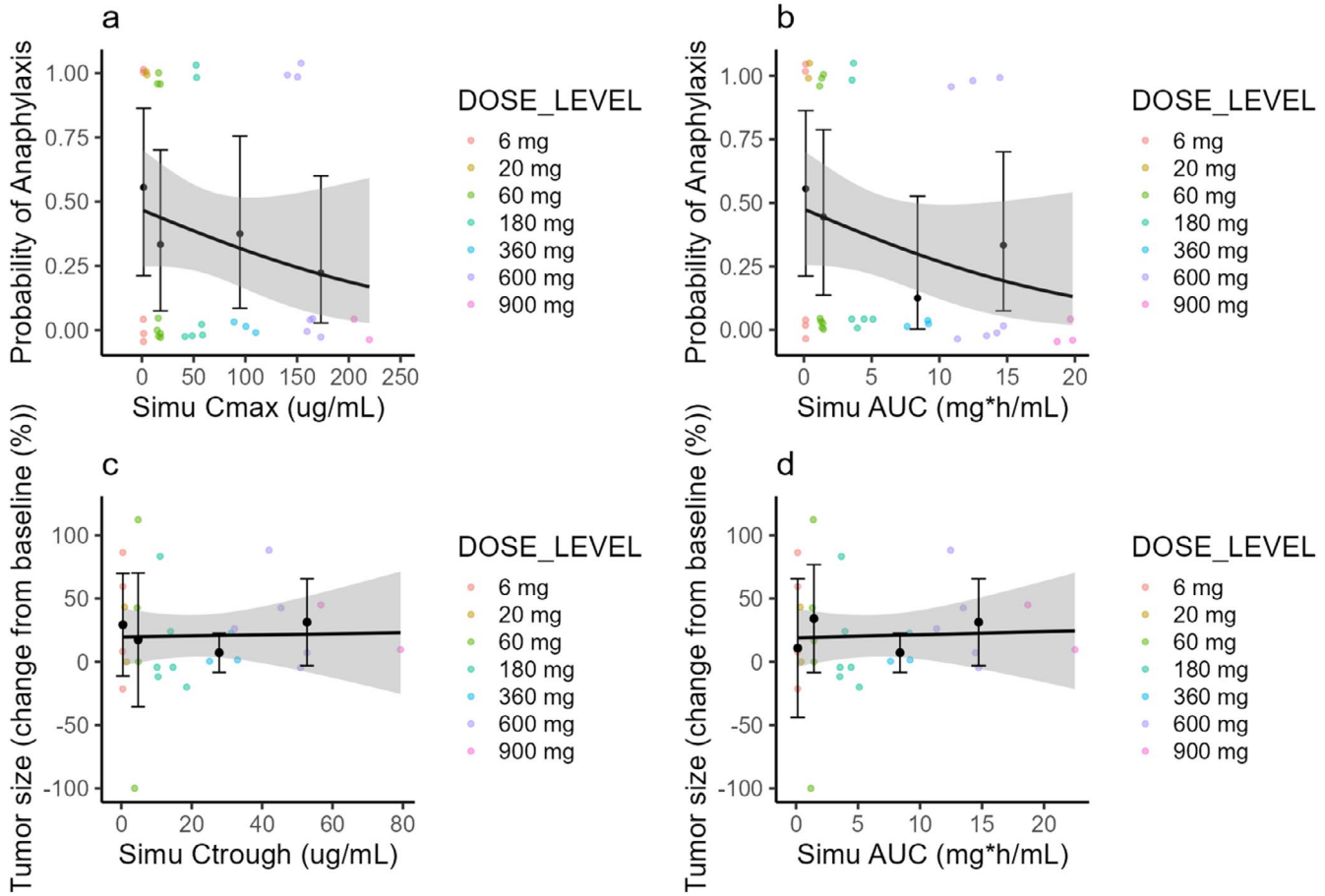

FIGURE 6 | AEs and efficacy versus exposure metrics, (a) the relationship between C_{max} and anaphylaxis of curve, (b) the relationship between AUC and anaphylaxis of curve, (c) the relationship between C_{trough} and tumor size of curve, (d) the relationship between AUC and tumor size of curve. Line represents predicted probability. Shaded area corresponds to 95% CIs.

treatment [31, 32]. In contrast to previous reports on other PD-1 inhibitors, body weight was not identified as a statistically significant covariate impacting the PK parameters of Fanastomig in this study. This suggests that fixed dosing of Fanastomig is appropriate.

The GOF plots indicate some underprediction for observations >140 μg/mL, representing approximately 5% of the dataset. Notably, concentrations exceeding 140 μg/mL were observed only at doses ≥600 mg. This underprediction bias could potentially be attributed to factors such as inaccurate PK sampling sites (e.g., collecting PK samples from the same arm as the infusion site, contrary to the clinical protocol). Additionally, the limited sample size in this concentration range may have contributed to the model's inability to accurately capture these higher concentrations. Despite this observation, the bias is not considered clinically meaningful. This model might be further modified and validated after accumulating more data in future clinical trials.

PD-1 has predominant cell surface expression, which is displayed persistently at the cell surface [15]. The EC_{50}-derived E_{max} model for anti-PD-1 peripheral RO is about 0.084 μg/mL, which was observed with a limited sample size as one caveat.

Based on the PK and RO data, two additional less-frequent dosing regimens were proposed. These dosing adjustments aim to assess the feasibility and potential patient benefits regarding compliance and therapeutic outcomes. The specific dosing regimens require further exploration in a larger patient population. The rationale behind this approach is that a flexible dosing strategy may alleviate the burden on patients and maximize the benefit/risk ratio while maintaining the desired pharmacological effect. The goal was to identify an optimal dosing regimen that balances effectiveness and safety, thereby enhancing adherence and overall treatment success.

A higher incidence of ADA was observed among patients. Despite the elevated titer, no significant impact on PK parameters such as CL or V (data not shown) was observed. This suggests that the presence of ADA does not necessarily correlate with reduced drug efficacy or altered PK in this patient population. The most frequent treatment-related AEs were IRR, fatigue, and diarrhea. Although fatigue and diarrhea occurred in a small percentage of patients (<15% for any grade), this frequency does not warrant further detailed analysis. Interestingly, a strong correlation was observed between the maximum ADA titer and anaphylaxis. Conversely, an inverse relationship between maximum ADA titer and the administered dose was noted, suggesting that a higher dosing regimen might mitigate the effect of ADA on anaphylaxis. Therefore, relatively higher dose regimens are proposed for further development to explore an optimized benefit/risk profile. No significant ER relationship

between any Fanastomig exposure metrics and tumor size was observed in the limited number of patients.

In conclusion, the evaluation of PD-1 RO and the corresponding target concentration of Fanastomig in tumors provides a rationale for the recommended therapeutic dosing regimen for Fanastomig monotherapy. This dosing regimen did not cause any safety risks based on the safety–exposure analysis, and a preliminary efficacy signal was observed. These findings may offer an optimization of the benefit/risk ratio in potential indications.

Author Contributions

C.J. wrote the manuscript. All authors designed and performed the research. C.J. analyzed the data. All authors critically reviewed the manuscript and approved the final version for publication.

Acknowledgments

We would like to express our sincere gratitude to the patients and their families who participated in this study. We also acknowledge the significant contributions of the investigators, research nurses, study coordinators, and operational staff involved in this project.

Conflicts of Interest

C.J., F.R., M.Z., Q.L., and Y.Z. are employees of Shanghai EpimAb Biotherapeutics Co., Ltd, and S.Z., G.Y. are former employees of Shanghai EpimAb Biotherapeutics Co., Ltd. The authors declare no conflicts of interest.

References

1. A. Mishra, S. C. Sarangi, and K. Reeta, "First-In-Human Dose: Current Status Review for Better Future Perspectives," *European Journal of Clinical Pharmacology* 76 (2020): 1237–1243.

2. C. Guo, K. H. Liao, M. Li, et al., "PK/PD Model-Informed Dose Selection for Oncology Phase I Expansion: Case Study Based on PF-06939999, a PRMT5 Inhibitor," *CPT: Pharmacometrics & Systems Pharmacology* 12 (2023): 1619–1625.

3. J. Van Gerven and M. Bonelli, "Commentary on the EMA Guideline on Strategies to Identify and Mitigate Risks for First-In-Human and Early Clinical Trials With Investigational Medicinal Products," *British Journal of Clinical Pharmacology* 84 (2018): 1401–1409.

4. H. Moon, "FDA Initiatives to Support Dose Optimization in Oncology Drug Development: The Less May be the Better," *Translational Clinical and Pharmacology* 30 (2022): 71–74.

5. EFPIA MID3 Workgroup, S. F. Marshall, R. Burghaus, et al., "Good Practices in Model-Informed Drug Discovery and Development: Practice, Application, and Documentation," *CPT: Pharmacometrics & Systems Pharmacology* 5 (2016): 93–122.

6. A. Mercier, S. Ueckert, M. Sunnåker, et al., "From Plan to Pivot: How Model-Informed Drug Development Shaped the Dose Strategy of the Zibotentan/Dapagliflozin *ZENITH* Trials," *Clinical Pharmacology and Therapeutics* 116 (2024): 653–664.

7. S. Marshall, M. Ahamadi, J. Chien, et al., "Model-Informed Drug Development: Steps Toward Harmonized Guidance," *Clinical Pharmacology and Therapeutics* 114 (2023): 954–959.

8. R. Murphy, S. Halford, and S. N. Symeonides, "Project Optimus, an FDA Initiative: Considerations for Cancer Drug Development Internationally, From an Academic Perspective," *Frontiers in Oncology* 13 (2023): 1144056.

9. M. L. Johnson, F. Braiteh, J. E. Grilley-Olson, et al., "Assessment of Subcutaneous vs. Intravenous Administration of Anti–PD-1 Antibody PF-06801591 in Patients With Advanced Solid Tumors: A Phase 1 Dose-Escalation Trial," *JAMA Oncology* 5 (2019): 999–1007.

10. S. Agrawal, Y. Feng, A. Roy, G. Kollia, and B. Lestini, "Nivolumab Dose Selection: Challenges, Opportunities, and Lessons Learned for Cancer Immunotherapy," *Journal for Immunotherapy of Cancer* 4 (2016): 72.

11. H. Mo, J. Huang, J. Xu, et al., "Safety, Anti-Tumour Activity, and Pharmacokinetics of Fixed-Dose SHR-1210, an Anti-PD-1 Antibody in Advanced Solid Tumours: A Dose-Escalation, Phase 1 Study," *British Journal of Cancer* 119 (2018): 538–545.

12. J. R. Brahmer, S. S. Tykodi, L. Q. Chow, et al., "Safety and Activity of Anti–PD-L1 Antibody in Patients With Advanced Cancer," *New England Journal of Medicine* 366 (2012): 2455–2465.

13. C. Maritaz, S. Broutin, N. Chaput, A. Marabelle, and A. Paci, "Immune Checkpoint-Targeted Antibodies: A Room for Dose and Schedule Optimization?," *Journal of Hematology & Oncology* 15 (2022): 6.

14. A. Patnaik, S. P. Kang, D. Rasco, et al., "Phase I Study of Pembrolizumab (MK-3475; Anti–PD-1 Monoclonal Antibody) in Patients With Advanced Solid Tumors," *Clinical Cancer Research* 21 (2015): 4286–4293.

15. Food Drug Administration, "Pharmacokinetic-Based Criteria for Supporting Alternative Dosing Regimens of Programmed Cell Death Receptor-1 (Pd-1) or Programmed Cell Death-Ligand 1 (Pd-L1) Blocking Antibodies for Treatment of Patients With Cancer: Guidance for Industry—Fda Digital Collections," (2022), https://www.fda.gov.

16. A. Lindauer, C. R. Valiathan, K. Mehta, et al., "Translational Pharmacokinetic/Pharmacodynamic Modeling of Tumor Growth Inhibition Supports Dose-Range Selection of the Anti-PD-1 Antibody Pembrolizumab: Translational Pharmacokinetic/Pharmacodynamic Modeling," *CPT: Pharmacometrics & Systems Pharmacology* 6 (2017): 11–20.

17. J. Fu, F. Wang, L. H. Dong, et al., "Receptor Occupancy Measurement of Anti-PD-1 Antibody Drugs in Support of Clinical Trials," *Bioanalysis* 11 (2019): 1347–1358.

18. L. Zhu, M. Jiang, H. Wang, et al., "A Narrative Review of Tumor Heterogeneity and Challenges to Tumor Drug Therapy," *Annals of Translational Medicine* 9 (2021): 1351.

19. J. J. Luke, M. R. Patel, G. R. Blumenschein, et al., "The PD-1- and LAG-3-Targeting Bispecific Molecule Tebotelimab in Solid Tumors and Hematologic Cancers: A Phase 1 Trial," *Nature Medicine* 29 (2023): 2814–2824.

20. T. Schlothauer, S. Herter, C. F. Koller, et al., "Novel Human IgG1 and IgG4 Fc-Engineered Antibodies With Completely Abolished Immune Effector Functions," *Protein Engineering, Design & Selection* 29 (2016): 457–466.

21. C. Liu, J. Yu, H. Li, et al., "Association of Time-Varying Clearance of Nivolumab With Disease Dynamics and Its Implications on Exposure Response Analysis," *Clinical Pharmacology and Therapeutics* 101 (2017): 657–666.

22. J. J. Wilkins, B. Brockhaus, H. Dai, et al., "Time-Varying Clearance and Impact of Disease State on the Pharmacokinetics of Avelumab in Merkel Cell Carcinoma and Urothelial Carcinoma," *CPT: Pharmacometrics & Systems Pharmacology* 8 (2019): 415–427.

23. M. Marchand, R. Zhang, P. Chan, et al., "Time-Dependent Population PK Models of Single-Agent Atezolizumab in Patients With Cancer," *Cancer Chemotherapy and Pharmacology* 88 (2021): 211–221.

24. K. Ogasawara, K. Newhall, S. E. Maxwell, et al., "Population Pharmacokinetics of an Anti-PD-L1 Antibody, Durvalumab in Patients With Hematologic Malignancies," *Clinical Pharmacokinetics* 59 (2020): 217–227.

25. R. Bawa, J. Szebeni, T. J. Webster, and G. F. Audette, eds., "Immunogenicity Assessment for Therapeutic Protein Products 1," in *Immune*

Aspects of Biopharmaceuticals and Nanomedicines (Jenny Stanford Publishing, 2019), 537–583, https://doi.org/10.1201/b22372-17.

26. G. Shankar, S. Arkin, L. Cocea, et al., "Assessment and Reporting of the Clinical Immunogenicity of Therapeutic Proteins and Peptides—Harmonized Terminology and Tactical Recommendations," *AAPS Journal* 16 (2014): 658–673.

27. D. K. Shah and A. M. Betts, "Towards a Platform PBPK Model to Characterize the Plasma and Tissue Disposition of Monoclonal Antibodies in Preclinical Species and Human," *Journal of Pharmacokinetics and Pharmacodynamics* 39 (2012): 67–86.

28. R. Deng, D. Bumbaca, C. V. Pastuskovas, et al., "Preclinical Pharmacokinetics, Pharmacodynamics, Tissue Distribution, and Tumor Penetration of Anti-PD-L1 Monoclonal Antibody, an Immune Checkpoint Inhibitor," *MAbs* 8 (2016): 593–603.

29. D. Austin, M. Melhem, Y. Gandhi, S. Lu, and S. Visser, "Comparative Analysis of PD-1 Target Engagement of Dostarlimab and Pembrolizumab in Advanced Solid Tumors Using Ex Vivo IL-2 Stimulation Data," *CPT: Pharmacometrics & Systems Pharmacology* 12 (2023): 87–94.

30. G. Bajaj, X. Wang, S. Agrawal, et al., "Model-Based Population Pharmacokinetic Analysis of Nivolumab in Patients With Solid Tumors," *CPT: Pharmacometrics & Systems Pharmacology* 6 (2017): 58–66.

31. M. Melhem, E. Hanze, S. Lu, O. Alskär, S. Visser, and Y. Gandhi, "Population Pharmacokinetics and Exposure–Response of Anti-Programmed Cell Death Protein-1 Monoclonal Antibody Dostarlimab in Advanced Solid Tumours," *British Journal of Clinical Pharmacology* 88 (2022): 4142–4154.

32. M. Centanni, D. J. A. R. Moes, I. F. Trocóniz, J. Ciccolini, and J. G. C. Van Hasselt, "Clinical Pharmacokinetics and Pharmacodynamics of Immune Checkpoint Inhibitors," *Clinical Pharmacokinetics* 58 (2019): 835–857.

33. J. Elassaiss-Schaap, S. Rossenu, A. Lindauer, et al., "Using Model-Based 'Learn and Confirm' to Reveal the Pharmacokinetics-Pharmacodynamics Relationship of Pembrolizumab in the KEYNOTE-001 Trial," *CPT: Pharmacometrics & Systems Pharmacology* 6 (2017): 21–28.

Supporting Information

Additional supporting information can be found online in the Supporting Information section.